SWAP Gate between a Majorana Qubit and a Parity-Protected Superconducting Qubit

Luca Chirolli,[1,2] Norman Y. Yao,[1,3] and Joel E. Moore[1,4]
[1]Department of Physics, University of California Berkeley, Berkeley, California 94720, USA
[2]Istituto Nanoscienze—CNR, I-56127 Pisa, Italy
[3]Department of Physics, Harvard University, Cambridge, Massachusetts 02138, USA
[4]Materials Sciences Division, Lawrence Berkeley National Laboratory, Berkeley, California 94720, USA

(Received 7 May 2022; accepted 15 September 2022; published 20 October 2022)

High fidelity quantum information processing requires a combination of fast gates and long-lived quantum memories. In this Letter, we propose a hybrid architecture, where a parity-protected superconducting qubit is directly coupled to a Majorana qubit, which plays the role of a quantum memory. The superconducting qubit is based upon a π-periodic Josephson junction realized with gate-tunable semiconducting wires, where the tunneling of individual Cooper pairs is suppressed. One of the wires additionally contains four Majorana zero modes that define a qubit. We demonstrate that this enables the implementation of a SWAP gate, allowing for the transduction of quantum information between the topological and conventional qubit. This architecture combines fast gates, which can be realized with the superconducting qubit, with a topologically protected Majorana memory.

DOI: 10.1103/PhysRevLett.129.177701

Introduction.—Majorana zero-energy modes (MZMs) [1–5] realized in condensed matter systems [6–14] are localized at far ends of the system and are expected to be robust with respect to local perturbations. Topologically protected Majorana qubits (MQs) encoded in MZM are hardly disturbed by an environment that acts locally and are expected to show very long coherence times [3]. Several schemes for topologically protected quantum information processing based upon MZMs have been proposed [15–22]. An alternative route, which may be particularly relevant in the noisy intermediate-scale quantum technology era [23], is to envision a hybrid architecture combining topologically protected memories with conventional qubits [24–26]. In this context, a MQ could serve as a quantum memory or quantum buffer and a key ingredient is provided by a SWAP gate that enables quantum state swapping between an "ordinary" qubit and a topologically protected memory.

Superconducting qubits are a particularly natural candidate since solid state realizations of MZMs typically involve a parent superconductor and are often based on proximity-induced topological superconductivity. Early suggestions for interactions between a superconducting qubit and a MQ were based on a number of different schemes, including coupling to a flux qubit [27,28], a flux qubit based readout [29,30], a top-transmon in which MZMs are moved between the islands of a transmon so to implement a parity-protected scheme [31], and a fluxonium based on the 4π-Josephson effect, where a MQ generates avoided crossing in the spectrum [32]. Other approaches based on transmons have been recently put forward, suggesting to encode the fermion parity in the cavity dispersive shift [33,34], or to use the microwave spectrum to detect the presence of MZMs [35,36]. In this context, the role of Coulomb effects on an island hosting MZMs has also been recently considered [37].

In this Letter, we study the coupling between a parity-protected superconducting qubit (PPSQ) and a MQ and we present a setup that enables the implementation of a SWAP gate between the two. A PPSQ is constituted by a superconducting island coupled to a reference circuit by a π-periodic Josephson junction (JJ) described by a $\cos(2\varphi)$ energy-phase relation. The latter captures the tunneling of pairs of Cooper pairs at the junction and preserves the parity of the Cooper pair number on the island. The MQ is formed through four MZMs: two of which contained in the superconducting island, the other two in the bulk reference, and their coupling at the junction is provided by the 4π-periodic Josephson effect. In such a combined system, in the weak charging regime the charging energy of the superconducting qubit can distinguish the presence of a single electron in the island, thus resolving the two states of the MQ. In addition, the coupling via the 4π-periodic Josephson effect enables the implementation of a SWAP gate without need of braiding operations on the MQ. In the weak transmon regime the protocol well adapts to Andreev qubits [38].

An experimental realization of an effective $\cos(2\varphi)$ relation has been a long-standing goal and only recently have PPSQs been realized. Relevant implementations are based on rhombi of four nominally equal JJs [39–43], ladders of JJs realizing a current-mirror $0-\pi$ qubit [44], gatemons realized through semiconducting wires [45–48], and superinductors obtained through chains of JJs [49–51]. The use of $\cos(2\varphi)$ Josephson relations have recently been proposed as a tool for modulating the Josephson potential

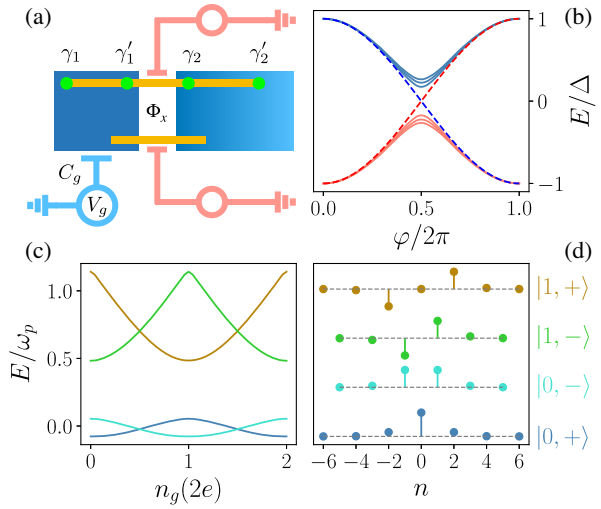

FIG. 1. (a) Circuit of a PPSQ coupled to a MQ. (b) Particle-hole symmetric subgap spectrum of a gate-tunable JJ containing a Majorana bound state and three Andreev bound states. (c) Spectrum showing the four lowest energy states, versus offset charge $n_g = C_g V_g/(2e)$, for $E_J/E_C = 6$ and in units of $\omega_p = \sqrt{32 E_J E_C}$. (d) Associated wave functions $|k,\tau\rangle$, specified by principal quantum number k and parity $\tau = \pm$, in the charge basis showing the even and odd number content.

and enhancing coherence times through band engineering [52]. We focus on the gatemon-based realization, but the protocol is general and can be realized through any implementation of PPSQs.

The system.—We consider the system shown in Fig. 1(a) consisting of a superconducting island coupled to a reference superconductor via two semiconducting wires that form two gate-tunable JJs [46,47]. One of the two wires is assumed to realize a topological superconductor [6,7] and it is cut in two segments, each hosting a pair of MZMs at its ends, γ_i and γ_i' for $i = 1, 2$. The modes γ_1' and γ_2 overlap across the junction and produce a bound state whose energy depends on the gauge invariant superconducting phase difference φ via the 4π-periodic Josephson effect, as shown by the dashed lines in Fig. 1(b). The two segments are assumed to be much longer than the superconducting coherence length, so that no hybridization takes place between γ_i and γ_i' in each segment. At the same time, we keep in the description finite hybridization energies λ_i, that well describe the case of an Andreev qubit. The Hamiltonian describing the coupling among the four MZMs reads

$$H_{\mathrm{MZM}} = i\gamma_1'\gamma_2 E_M \cos(\varphi/2) + i\lambda_1\gamma_1\gamma_1' + i\lambda_2\gamma_2\gamma_2', \quad (1)$$

with E_M the bare coupling at the junction.

In addition to the MZMs, the two semiconducting wires are assumed to host also highly transparent Andreev bound states, that in the absence of magnetic field are described by an energy-phase relation $\mathcal{U}_i(\varphi_i) = -\Delta \sum_n \sqrt{1 - T_n^{(i)} \sin^2(\varphi_i/2)}$, with $i = 1, 2$ labeling the two wires, Δ the induced superconducting gap on the wires [37], $T_n^{(i)}$ the transmission coefficient of the nth conducting channel, and φ_i the gauge-invariant phase difference across the ith junction. The particle-hole symmetric subgap spectrum of the topological junction is schematically shown in Fig. 1(b), where the Andreev states (continuous lines) and the Majorana states (dashed lines) are shown together. We assume the Andreev and the Majorana state to be independently tunable through applied electrostatic gates. A more precise tuning can be experimentally achieved through a parallel of three wires [53], one of which realizes a topological superconductor.

Parity-protected superconducting qubit.—The parallel of two wires yields the effective Josephson energy-phase relation $\mathcal{U}(\varphi) = \mathcal{U}_1(\varphi) + \mathcal{U}_2(\varphi_x - \varphi)$, with $\varphi_x = 2\pi\Phi_x/\Phi_0$ the flux threading the loop in units of $\Phi_0 = h/2e$. It has been shown in Ref. [48] that by setting $\mathcal{U}_1 = \mathcal{U}_2$ and $\varphi_x = \pi$ all odd harmonics are suppressed and the junction realizes a π-periodic energy-phase relation [54]. Focusing on the second harmonic and neglecting all other exponentially suppressed harmonics, the Hamiltonian of the PPSQ is specified by the Josephson energy and the charging energy and reads

$$H_0 = 4E_C(\hat{n} - n_g)^2 - E_J \cos(2\hat{\varphi}). \quad (2)$$

The gauge invariant phase difference $\hat{\varphi}$ and the number of Cooper pairs $\hat{n}$ are conjugate variables satisfying $[\hat{\varphi}, \hat{n}] = i$. Here, E_J is the Josephson energy of the π-periodic element and $E_C = e^2/2C$ is the charging energy, with the total capacitance, $C = C_J + C_g$, given by the capacitance of the JJ, C_J, and the capacitance C_g of a side gate. The latter enables to control the average offset charge on the island $n_g = C_g V_g/(2e)$ through a voltage V_g.

In the charge basis the π-periodic Josephson term is written as $\cos(2\hat{\varphi}) = \frac{1}{2}\sum_n |n+2\rangle\langle n| + \mathrm{H.c.}$, and we clearly see that it does not couple states differing by an odd number of Cooper pairs in the superconducting island. We then define a conserved quantity, labeled by $\tau = \pm 1$, associated with the parity of the number of Cooper pairs in the island, which we term boson parity. The Hamiltonian of the PPSQ is written as $H_0 = H_+^0 + H_-^0$, where

$$H_\pm^0 = \sum_{n_\pm} 4E_C(n_\pm - n_g)^2 \mathbb{P}_{n_\pm} - \frac{E_J}{2}|n_\pm + 2\rangle\langle n_\pm| + \mathrm{H.c.}, \quad (3)$$

with $n_\pm$ even or odd, respectively, $\mathbb{P}_{n_\pm} = |n_\pm\rangle\langle n_\pm|$. The energy levels can be generally written as $E_k^\tau(n_g)$, with $k = 0, 1, 2, \ldots$ a principal quantum number. Deep in the charging regime characterized by $E_C \gg E_J$, the system is very sensitive to the presence of additional charge on the island. The sensitivity persists also in the weak charging regime, specified by $E_C/E_J \lesssim 1$, and the four lowest energy

levels and their associated wave functions are shown in Figs. 1(c) and 1(d), respectively, for $E_J/E_C = 6$. By inspection of Eq. (3) we see that a shift $n_g \to n_g + 2$ leaves the Hamiltonian invariant, resulting in an overall $4e$ periodicity of the spectrum, as shown in Fig. 1(b). The crossings at $n_g = \frac{1}{2}, \frac{3}{2}$ are protected by conservation of the boson parity. Focusing on the four lowest energy states, the Hamiltonian H_0 then reads

$$H_0 = \frac{\epsilon(n_g)}{2}\tau_z(1-\sigma_z) + \frac{1}{2}[E_{10} + \epsilon'(n_g)\tau_z](1+\sigma_z), \quad (4)$$

where the Pauli matrices σ_i span the $k = 0, 1$ states and the Pauli matrices τ_i span the boson parity states. In addition, we have $E_{10} = (E_1^+ + E_1^- - E_0^+ - E_0^-)/2$, $\epsilon = (E_0^- - E_0^+)/2$, $\epsilon' = (E_1^+ - E_1^-)/2$. In Fig. 1(c) deviations from a $\cos(\pi n_g)$ dependence, typical of the transmon regime [55], can be appreciated in the higher energy levels, allowing for independent tuning of ϵ and ϵ' by the offset charge. The PPSQ is provided by the two lowest energy states, corresponding to $\sigma_z = -1$, and in order to separate them from the rest of the spectrum and still keep sensitivity to the charge on the island an intermediate weak charging regime $E_C \lesssim E_J$ is required.

Coupling Hamiltonian.—We now consider the coupling between the MQ and the PPSQ. The full Hamiltonian reads $H = H_0 + H_{\mathrm{MZM}}$. To properly treat the MQ we introduce two fermionic operators, $c_i = (\gamma_i + i\gamma_i')/2$, that allow us to label states via their occupation number $|q_1, q_2\rangle$, with $\hat{q}_i = c_i^\dagger c_i$. In each sector of the total fermion parity $\mathcal{P} = e^{i\pi(\hat{q}_1+\hat{q}_2)}$ the four MZMs encode a qubit degree of freedom [19]. We can introduce Pauli operators to span the qubit states, $\mathcal{P}\eta_x = i\gamma_1'\gamma_2$, $\eta_z = \hat{p}_1 = -i\gamma_1\gamma_1'$, and $\mathcal{P}\eta_z = \hat{p}_2 = -i\gamma_2\gamma_2'$. The presence of MZMs in the superconducting island affects the spectrum of the system through a constraint in the wave function, that becomes antiperiodic in case an odd number of electrons is present in the island, $\Psi(\varphi + 2\pi n) = (-)^{n\hat{q}_1}\Psi(\varphi)$ [56]. By performing the unitary transformation $H \to U^\dagger H U$, with $U = e^{i\varphi\hat{q}_1/2}$ [33,36,57,58], the Hamiltonian becomes

$$H = 4E_C(\hat{n} + \hat{q}_1/2 - n_g)^2 - E_J\cos(2\hat{\varphi}) - \lambda_1\hat{p}_1 - \lambda_2\hat{p}_2 + E_M[(c_1c_2 - c_2^\dagger c_1)(1 + e^{i\hat{\varphi}/2}) + \mathrm{H.c.}]. \quad (5)$$

The coupling between the MQ and the PPSQ appears in two terms: (i) the charging energy and (ii) the hybridization term proportional to E_M. In each fermion parity sector the charge $\hat{q}_1$ takes the values 0,1 between the MQ states and the hybridization energy only differs for the sign of the coupling in the two fermion parity sectors.

Focusing on the even fermion parity sector ($\mathcal{P} = 1$) and taking matrix elements between the MQ states $|00\rangle, |11\rangle$ the Hamiltonian reads

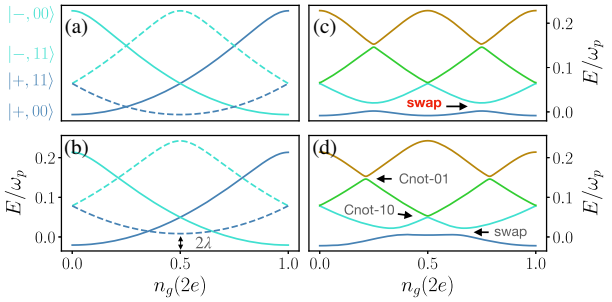

FIG. 2. Four lowest energy levels of the Hamiltonian Eq. (6) as a function of n_g for equal JJs, $\varphi_x = \pi$, and $E_J/E_C \simeq 6$. (a) $\lambda = E_M = 0$. (b) $\lambda = 0.2E_C$ and $E_M = 0$. (c) A finite $E_M = 0.2E_C$ splits the crossings at $n_g = 0, 1/4, 1/2, 3/4$ and results in a e-periodic spectrum. (d) A finite λ shifts the avoided crossing from $n_g = 1/4, 3/4$ and results in a $2e$-periodic spectrum. The three avoided crossings allow for two C-NOT gates and a SWAP gate, as indicated.

$$H(n_g) = \begin{pmatrix} H_0(n_g) - \lambda & E_M(1 + e^{i\hat{\varphi}})/2 \\ E_M(1 + e^{-i\hat{\varphi}})/2 & H_0(n_g - 1/2) + \lambda \end{pmatrix}. \quad (6)$$

In the diagonal blocks, in addition to the shift in the offset charge, a further energy imbalance is provided by the hybridization energy of the MZMs, $\lambda = \lambda_1 + \lambda_2$. The four lowest energy states associated to the two bosonic parity states and the two MQ states are $|\psi_{n_g}^{\pm}\rangle|00\rangle$ and $|\psi_{n_g-1/2}^{\pm}\rangle|11\rangle$ and their energies as a function of n_g are shown in Fig. 2(a) for the choice $E_J \simeq 6E_C$, in the weak charging regime [59]. By switching on a finite λ the $|11\rangle$ states shift up in energy with respect to the $|00\rangle$ states, as shown in Fig. 2(b). The periodicity versus the offset charge is still $4e$, as no coupling is present between the different states. In Fig. 2(c) a finite E_M opens a splitting between all crossing producing a change in the periodicity from $4e$ to e in the offset charge. In Fig. 2(d), by simultaneously switching on both λ and E_M we see that the periodicity of the spectrum becomes $2e$.

The effect of the coupling parametrized by E_M and λ is best appreciated in the microwave spectrum (MWS) of a nearby capacitively coupled microwave cavity. The offset charge acquires a time dependence $n_g \to n_g + \delta n_g(t)$ that gives rise to a coupling $\delta n_g(t)(\hat{n} + \hat{q}_1/2)$. Assuming the system initially in the ground state $|0\rangle$, the linear response MWS is given by $S(\omega) = \sum_{p>0}|\langle p|(\hat{n} + \hat{q}_1/2)|0\rangle|^2\delta(\omega - \omega_{0p})$, with $|p\rangle$ all eigenstates of the Hamiltonian Eq. (6) and $\omega_{0p} = \omega_p - \omega_0$. In the absence of MZMs the ground state switches boson parity with period $2e$. The MWS is shown in Fig. 3 for $E_M = 0.2E_C$ and different values of λ. In Fig. 3(a) we see that a finite E_M yields a e-periodic spectrum compatible with the avoided crossings between the energy levels shown in Fig. 2(c). In Figs. 3(b) and 3(c) a finite λ breaks the e periodicity and

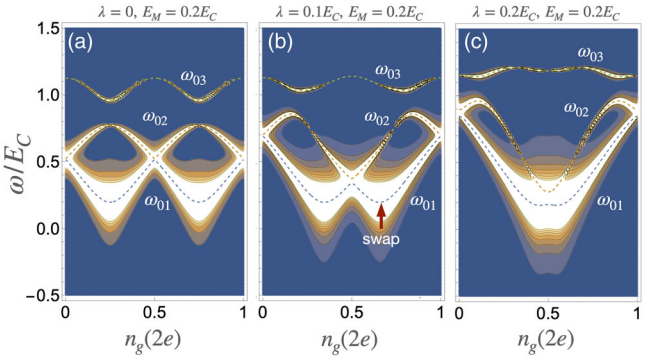

FIG. 3. Microwave spectrum $S(\omega)$ of the coupled system in the weakly transmon regime, for $E_J/E_C = 10$ and $E_M = 0.2E_C$. (a) $\lambda = 0$ showing e-periodic transitions. A finite $\lambda = 0.1$ (b) and $\lambda = 0.2E_C$ (c) produce a $2e$-periodic spectrum.

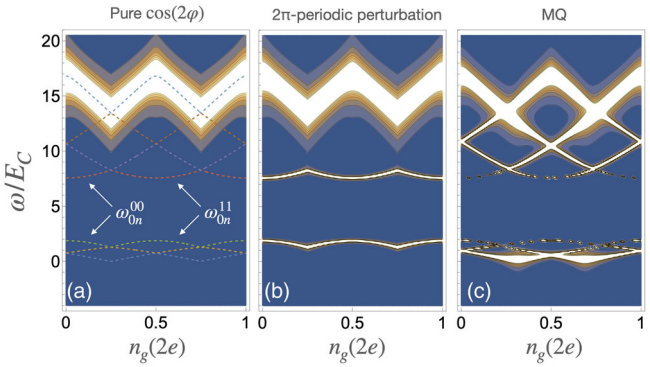

FIG. 4. Microwave spectrum of a PPSQ: (a) with a pure π-periodic potential, (b) in presence of 2π-periodic perturbations, and (c) with a MZMs in one junction. The part of the spectrum between $-0.5 < \omega/E_C < 1.5$ corresponds to Fig. 3(b).

restores a $2e$-periodic spectrum compatible with the one shown in Fig. 2(d).

SWAP gate.—We can write an effective low energy qubit-qubit Hamiltonian by taking matrix elements of the Hamiltonian Eq. (6) between the four lowest energy levels, $|\psi^{\pm}_{n_g}\rangle|00\rangle$ and $|\psi^{\pm}_{n_g-1/2}\rangle|11\rangle$, of the Hamiltonian H_0. The relevant matrix elements induced by the MQ are $g_{\tau,\tau'}(n_g) = \frac{1}{2}\langle\psi^{\tau}_{n_g}|(1+e^{i\hat{\varphi}})|\psi^{\tau'}_{n_g-1/2}\rangle$, and in the weak charging regime they have a weak dependence on n_g. Introducing Pauli matrices η_i spanning the MQ subspace, the qubit-qubit Hamiltonian at $n_g = 3/4$ reads

$$H = \Omega\tau_z + (\omega_M - \lambda)\eta_z + \delta\eta_z\tau_z + E_M(g_{-,+}\eta^+\tau^- + g_{+,-}\eta^+\tau_+ + g_{+,+}\eta^+ + \text{H.c.}), \quad (7)$$

where $g_{\tau,\tau'}$, $\Omega = \mathrm{Tr}[H\tau_z]/4$, $\omega_M = \mathrm{Tr}[H\eta_z]$, and $\delta = \mathrm{Tr}[H\tau_z\eta_z]/4$ are calculated at $n_g = 3/4$ [60]. This is the most important result of the present Letter: it shows that a coupling between a PPSQ and a MQ is possible and can be controlled by E_M. In the weak charging regime, the coupling $g_{\tau,\tau'}$ are all different and the Hamiltonian enables the implementation the SWAP gate also deep in the topological phase $\lambda = 0$. At $E_M = 0$ and $n_g = 1/4$ the qubits are decoupled. By tuning the offset charge at $n_g = 3/4$ [see Fig. 2(c)] and by switching on E_M for a time $T = \pi m/(g_{+,-}E_M)$, with m integer, a SWAP gate can be obtained with high fidelity, with deviation from $F = 1$ due to failure of the rotating wave approximation, which is guaranteed only for $g_{+,-}E_M \ll \delta$. A full protocol for the SWAP gate is presented in the Supplemental Material [61]. This is a very important result, as it shows that a SWAP gate can be performed without recourse to braiding. In the weak transmon regime we have that $\omega_M = 0$ and $g_{\tau,\tau'} = g$, and a finite λ is necessary to achieve a SWAP gate by actively driving the flip-flop term $|+,11\rangle\langle-,00|$ at a frequency $\omega = 2(\Omega - \lambda)$. In addition, for constant E_M the hybridization between the two qubits allows for two C-NOT and a SWAP gate between the hybridized eigenstates. Deviations may still arise due to failure of the rotating wave approximation, so that weak values of E_M are required. This regime well applies to Andreev qubits.

2π-periodic perturbations.—The ability to engineer a π-periodic JJ is crucial for the definition of a well-behaved PPSQ and 2π-periodic perturbations may occur in experiments. The minima of the $\cos(2\varphi)$ potential at $\varphi = 0, \pi$ map into each other by the mirror transformation $M_\varphi : \varphi \to \pi - \varphi$. Even and odd perturbations under M_φ, such as $\sin(\varphi)$ and $\cos(\varphi)$, respectively, have a different impact. An odd perturbation couples states of the same k and opposite τ yielding $\alpha_k = \langle k,-|\cos(\varphi)|k,+\rangle$, that produces an energy imbalance between the two minima. States of opposite parity that differ by one unit of k are not coupled. An even perturbation cannot couple opposite parity states of the same k, $\langle k,+|\sin(\varphi)|k,-\rangle = 0$, and does not generate an energy imbalance. Nevertheless, it can couple states that differ by one unit of k and of opposite parity, giving rise to finite matrix elements $\beta_\pm = \langle 0,\pm|\sin(\varphi)|1,\mp\rangle$. A generic 2π-periodic perturbation acts as

$$H' = u_o(\alpha_+ - \alpha_-\sigma_z)\tau_x + u_e\beta\sigma_x\tau_x \quad (8)$$

with $u_{e/o}$ the amplitude of the even/odd perturbation and $\alpha_\pm = (\alpha_0 \pm \alpha_1)/2$. In Fig. 4(a) the microwave spectrum is shown for a pure π-periodic Hamiltonian H_0 with $\lambda = E_M = 0$. No transitions are allowed in the frequency window $-0.5 < \omega/E_C < 1.5$. The effect of a 2π-periodic perturbation containing both a $\cos(\varphi)$ and $\sin(\varphi)$ term is shown in Fig. 4(b), showing the transitions activated by the perturbation. The two branches associated with even and odd total number of fermions in the island are usually seen in the MWS as a result of an out-of-equilibrium population of the two fermion parity sectors. Finally, in Fig. 4(c) the presence of finite $E_M = 0.2E_C$ and $\lambda = 0.1E_C$ shows the activation of MQ induced transitions. It follows that the

presence of MZMs can be detected through MWS [62], even in presence of weak 2π-periodic perturbations.

Discussion.—We have shown how a MQ can be coupled to a PPSQ based on an effective π-periodic JJ. The setup enables the implementation of a SWAP gate between the two qubits without recourse to braiding, thus promoting a Majorana qubit as a memory for storage. Finite single-Cooper-pair tunneling has a detrimental effect on the SWAP gate, in that it reduces the regime of validity of the rotating wave approximation (see Ref. [61]). The dependence of the PPSQ Hamiltonian on the offset charge is particularly pronounced in the weak charging regime and the fidelity of the SWAP gate may acquire a typical Gaussian decay controlled by a dephasing rate Γ_ϕ. For gate times $T \ll 1/\Gamma_\phi$ the gate is robust to dephasing. A PPSQ can be also realized through a π junction [63] or through any other implementation, rendering the protocol and the results general.

The authors acknowledge very useful discussions with M. Carrega, A. Crippa, M. Devoret, V. Fatemi, E. Lee, and V. Manucharyan, and especially thank B. van Heck and R. Aguado for a careful reading of the manuscript and for comments about the evolution of Andreev states in magnetic field. This project has received funding from the European Union's Horizon 2020 research and innovation programme under the Marie Sklodowska-Curie Grant Agreement No. 841894. J. E. M. was supported by the U.S. Department of Energy, Office of Science through the Quantum Science Center (QSC), a National Quantum Information Science Research Center. N. Y. Y. was supported by the U.S. Department of Energy, Office of Science, through the Quantum Systems Accelerator (QSA), a National Quantum Information Science Research Center and the David and Lucile Packard foundation.

[1] E. Majorana, Teoria simmetrica dell'elettrone e del positrone, Il Nuovo Cimento (1924-1942) **14**, 171 (2008).
[2] N. Read and D. Green, Paired states of fermions in two dimensions with breaking of parity and time-reversal symmetries and the fractional quantum Hall effect, Phys. Rev. B **61**, 10267 (2000).
[3] A. Y. Kitaev, Unpaired Majorana fermions in quantum wires, Phys. Usp. **44**, 131 (2001).
[4] D. A. Ivanov, Non-Abelian Statistics of Half-Quantum Vortices in p-Wave Superconductors, Phys. Rev. Lett. **86**, 268 (2001).
[5] F. Wilczek, Majorana returns, Nat. Phys. **5**, 614 (2009).
[6] R. M. Lutchyn, J. D. Sau, and S. Das Sarma, Majorana Fermions and a Topological Phase Transition in Semiconductor-Superconductor Heterostructures, Phys. Rev. Lett. **105**, 077001 (2010).
[7] Y. Oreg, G. Refael, and F. von Oppen, Helical Liquids and Majorana Bound States in Quantum Wires, Phys. Rev. Lett. **105**, 177002 (2010).
[8] J. Alicea, New directions in the pursuit of Majorana fermions in solid state systems, Rep. Prog. Phys. **75**, 076501 (2012).
[9] C. Beenakker, Search for Majorana fermions in superconductors, Annu. Rev. Condens. Matter Phys. **4**, 113 (2013).
[10] S. M. Albrecht, A. P. Higginbotham, M. Madsen, F. Kuemmeth, T. S. Jespersen, J. Nygård, P. Krogstrup, and C. M. Marcus, Exponential protection of zero modes in Majorana islands, Nature (London) **531**, 206 (2016).
[11] R. Aguado, Majorana quasiparticles in condensed matter, Nuovo Cimento Riv. Ser. **40**, 523 (2017).
[12] R. M. Lutchyn, E. P. A. M. Bakkers, L. P. Kouwenhoven, P. Krogstrup, C. M. Marcus, and Y. Oreg, Majorana zero modes in superconductor–semiconductor heterostructures, Nat. Rev. Mater. **3**, 52 (2018).
[13] E. Prada, P. San-Jose, M. W. A. de Moor, A. Geresdi, E. J. H. Lee, J. Klinovaja, D. Loss, J. Nygård, R. Aguado, and L. P. Kouwenhoven, From andreev to Majorana bound states in hybrid superconductor–semiconductor nanowires, Nat. Rev. Phys. **2**, 575 (2020).
[14] K. Flensberg, F. von Oppen, and A. Stern, Engineered platforms for topological superconductivity and Majorana zero modes, Nat. Rev. Mater. **6**, 944 (2021).
[15] S. Bravyi and A. Kitaev, Universal quantum computation with ideal clifford gates and noisy ancillas, Phys. Rev. A **71**, 022316 (2005).
[16] A. Kitaev, Fault-tolerant quantum computation by anyons, Ann. Phys. (Amsterdam) **303**, 2 (2003).
[17] S. Das Sarma, M. Freedman, and C. Nayak, Topologically Protected Qubits from a Possible Non-Abelian Fractional Quantum Hall State, Phys. Rev. Lett. **94**, 166802 (2005).
[18] M. Freedman, C. Nayak, and K. Walker, Towards universal topological quantum computation in the $\nu = \frac{5}{2}$ fractional quantum Hall state, Phys. Rev. B **73**, 245307 (2006).
[19] C. Nayak, S. H. Simon, A. Stern, M. Freedman, and S. Das Sarma, Non-Abelian anyons and topological quantum computation, Rev. Mod. Phys. **80**, 1083 (2008).
[20] S. D. Sarma, M. Freedman, and C. Nayak, Majorana zero modes and topological quantum computation, npj Quantum Inf. **1**, 15001 (2015).
[21] J. Alicea, Y. Oreg, G. Refael, F. von Oppen, and M. P. A. Fisher, Non-Abelian statistics and topological quantum information processing in 1d wire networks, Nat. Phys. **7**, 412 (2011).
[22] D. Aasen, M. Hell, R. V. Mishmash, A. Higginbotham, J. Danon, M. Leijnse, T. S. Jespersen, J. A. Folk, C. M. Marcus, K. Flensberg, and J. Alicea, Milestones Toward Majorana-Based Quantum Computing, Phys. Rev. X **6**, 031016 (2016).
[23] J. Preskill, Quantum Computing in the NISQ era and beyond, Quantum **2**, 79 (2018).
[24] M. A. Nielsen and I. L. Chuang, *Quantum Computation and Quantum Information: 10th Anniversary Edition* (Cambridge University Press, Cambridge, England, 2010).
[25] A. Y. Kitaev, A. H. Shen, and M. N. Vyalyi, *Classical and Quantum Computation* (American Mathematical Society, USA, 2002).
[26] J. Preskill, Fault-tolerant quantum computation, arXiv:quant-ph/9712048.

[27] L. Jiang, C. L. Kane, and J. Preskill, Interface Between Topological and Superconducting Qubits, Phys. Rev. Lett. **106**, 130504 (2011).

[28] P. Bonderson and R. M. Lutchyn, Topological Quantum Buses: Coherent Quantum Information Transfer Between Topological and Conventional Qubits, Phys. Rev. Lett. **106**, 130505 (2011).

[29] F. Hassler, A. R. Akhmerov, C.-Y. Hou, and C. W. J. Beenakker, Anyonic interferometry without anyons: How a flux qubit can read out a topological qubit, New J. Phys. **12**, 125002 (2010).

[30] C.-Y. Hou, F. Hassler, A. R. Akhmerov, and J. Nilsson, Probing Majorana edge states with a flux qubit, Phys. Rev. B **84**, 054538 (2011).

[31] F. Hassler, A. R. Akhmerov, and C. W. J. Beenakker, The top-transmon: A hybrid superconducting qubit for parity-protected quantum computation, New J. Phys. **13**, 095004 (2011).

[32] D. Pekker, C.-Y. Hou, V. E. Manucharyan, and E. Demler, Proposal for Coherent Coupling of Majorana Zero Modes and Superconducting Qubits Using the 4π Josephson Effect, Phys. Rev. Lett. **111**, 107007 (2013).

[33] E. Ginossar and E. Grosfeld, Microwave transitions as a signature of coherent parity mixing effects in the Majorana-transmon qubit, Nat. Commun. **5**, 4772 (2014).

[34] K. Yavilberg, E. Ginossar, and E. Grosfeld, Fermion parity measurement and control in Majorana circuit quantum electrodynamics, Phys. Rev. B **92**, 075143 (2015).

[35] J. Ávila, E. Prada, P. San-Jose, and R. Aguado, Majorana oscillations and parity crossings in semiconductor nanowire-based transmon qubits, Phys. Rev. Res. **2**, 033493 (2020).

[36] J. Ávila, E. Prada, P. San-Jose, and R. Aguado, Superconducting islands with topological Josephson junctions based on semiconductor nanowires, Phys. Rev. B **102**, 094518 (2020).

[37] D. Pikulin, K. Flensberg, L. I. Glazman, M. Houzet, and R. M. Lutchyn, Coulomb Blockade of a Nearly Open Majorana Island, Phys. Rev. Lett. **122**, 016801 (2019).

[38] M. Hays, V. Fatemi, D. Bouman, J. Cerrillo, S. Diamond, K. Serniak, T. Connolly, P. Krogstrup, J. Nygård, A. L. Yeyati, A. Geresdi, and M. H. Devoret, Coherent manipulation of an Andreev spin qubit, Science **373**, 430 (2021).

[39] G. Blatter, V. B. Geshkenbein, and L. B. Ioffe, Design aspects of superconducting-phase quantum bits, Phys. Rev. B **63**, 174511 (2001).

[40] B. Douçot and J. Vidal, Pairing of Cooper Pairs in a Fully Frustrated Josephson-Junction Chain, Phys. Rev. Lett. **88**, 227005 (2002).

[41] I. V. Protopopov and M. V. Feigel'man, Anomalous periodicity of supercurrent in long frustrated Josephson-junction rhombi chains, Phys. Rev. B **70**, 184519 (2004).

[42] S. Gladchenko, D. Olaya, E. Dupont-Ferrier, B. Douçot, L. B. Ioffe, and M. E. Gershenson, Superconducting nanocircuits for topologically protected qubits, Nat. Phys. **5**, 48 (2009).

[43] M. T. Bell, J. Paramanandam, L. B. Ioffe, and M. E. Gershenson, Protected Josephson Rhombus Chains, Phys. Rev. Lett. **112**, 167001 (2014).

[44] A. Kitaev, Protected qubit based on a superconducting current mirror, arXiv:cond-mat/0609441.

[45] G. de Lange, B. van Heck, A. Bruno, D. J. van Woerkom, A. Geresdi, S. R. Plissard, E. P. A. M. Bakkers, A. R. Akhmerov, and L. DiCarlo, Realization of Microwave Quantum Circuits using Hybrid Superconducting-Semiconducting Nanowire Josephson Elements, Phys. Rev. Lett. **115**, 127002 (2015).

[46] T. W. Larsen, K. D. Petersson, F. Kuemmeth, T. S. Jespersen, P. Krogstrup, J. Nygård, and C. M. Marcus, Semiconductor-Nanowire-Based Superconducting Qubit, Phys. Rev. Lett. **115**, 127001 (2015).

[47] F. Luthi, T. Stavenga, O. W. Enzing, A. Bruno, C. Dickel, N. K. Langford, M. A. Rol, T. S. Jespersen, J. Nygård, P. Krogstrup, and L. DiCarlo, Evolution of Nanowire Transmon Qubits and Their Coherence in a Magnetic Field, Phys. Rev. Lett. **120**, 100502 (2018).

[48] T. W. Larsen, M. E. Gershenson, L. Casparis, A. Kringhøj, N. J. Pearson, R. P. G. McNeil, F. Kuemmeth, P. Krogstrup, K. D. Petersson, and C. M. Marcus, Parity-Protected Superconductor-Semiconductor Qubit, Phys. Rev. Lett. **125**, 056801 (2020).

[49] P. Brooks, A. Kitaev, and J. Preskill, Protected gates for superconducting qubits, Phys. Rev. A **87**, 052306 (2013).

[50] W. C. Smith, A. Kou, X. Xiao, U. Vool, and M. H. Devoret, Superconducting circuit protected by two-Cooper-pair tunneling, Quantum Inf. **6**, 8 (2020).

[51] A. Gyenis, P. S. Mundada, A. Di Paolo, T. M. Hazard, X. You, D. I. Schuster, J. Koch, A. Blais, and A. A. Houck, Experimental realization of a protected superconducting circuit derived from the 0–π qubit, PRX Quantum **2**, 010339 (2021).

[52] L. Chirolli and J. E. Moore, Enhanced Coherence in Superconducting Circuits via Band Engineering, Phys. Rev. Lett. **126**, 187701 (2021).

[53] A. Ronzani, C. Altimiras, and F. Giazotto, Balanced double-loop mesoscopic interferometer based on Josephson proximity nanojunctions, Appl. Phys. Lett. **104**, 032601 (2014).

[54] Strictly speaking, an exact correspondence between energy and transmission eigenvalues is lost in the presence of an external magnetic field and a more complicated energy-phase relation is expected, with the appearance of odd terms such as $\sin(\varphi)$.

[55] J. Koch, T. M. Yu, J. Gambetta, A. A. Houck, D. I. Schuster, J. Majer, A. Blais, M. H. Devoret, S. M. Girvin, and R. J. Schoelkopf, Charge-insensitive qubit design derived from the cooper pair box, Phys. Rev. A **76**, 042319 (2007).

[56] L. Fu, Electron Teleportation via Majorana Bound States in a Mesoscopic Superconductor, Phys. Rev. Lett. **104**, 056402 (2010).

[57] B. van Heck, F. Hassler, A. R. Akhmerov, and C. W. J. Beenakker, Coulomb stability of the 4π-periodic Josephson effect of Majorana fermions, Phys. Rev. B **84**, 180502(R) (2011).

[58] A. Keselman, C. Murthy, B. van Heck, and B. Bauer, Spectral response of Josephson junctions with low-energy quasiparticles, SciPost Phys. **7**, 50 (2019).

[59] Calculations are done with the parallel of JJs realizing equal Andreev states for the choice $T_1^{(i)} = 0.96$, $T_2^{(i)} = 0.91$, $T_3^{(i)} = 0.9$, and $\Delta \simeq 72 E_C$.

[60] The trace is on the Hamiltonian Eq. (6) and in particular we have $\Omega(n_g)=(E_{00}^{+}-E_{00}^{-}+E_{11}^{+}-E_{11}^{-})/4$, $\omega_M(n_g)=(E_{00}^{+}+E_{00}^{-}-E_{11}^{+}-E_{11}^{-})/4$, and $\delta(n_g)=(E_{00}^{+}-E_{00}^{-}-E_{11}^{+}-E_{11}^{-})/4$, where $E_{11}^{\pm}(n_g)=E_{00}^{\pm}(n_g-1/2)$.

[61] See Supplemental Material at http://link.aps.org/supplemental/10.1103/PhysRevLett.129.177701 for presenting details of the SWAP gate and fidelity estimate.

[62] D. M. T. van Zanten, D. Sabonis, J. Suter, J. I. Väyrynen, T. Karzig, D. I. Pikulin, E. C. T. O'Farrell, D. Razmadze, K. D. Petersson, P. Krogstrup, and C. M. Marcus, Photon-assisted tunnelling of zero modes in a Majorana wire, Nat. Phys. **16**, 663 (2020).

[63] A. Bargerbos, M. Pita-Vidal, R. Žitko, J. Ávila, L. J. Splitthoff, L. Grünhaupt, J. J. Wesdorp, C. K. Andersen, Y. Liu, L. P. Kouwenhoven, R. Aguado, A. Kou, and B. van Heck, Singlet-doublet transitions of a quantum dot Josephson junction detected in a transmon circuit, PRX Quantum **3**, 030311 (2022).